Selenomethionine Quenching of Tryptophan Fluorescence Provides a Simple Probe of Protein Structure

*Matthew D. Watson [a]†, Ivan Peran [a]†, Junjie Zou [a,b], Osman Bilsel [c] and Daniel P. Raleigh [a,b,d]**

[a] Department of Chemistry, Stony Brook University, Stony Brook, New York 11794-3400, USA

[b] Laufer for Physical and Quantitative Biology, Stony Brook University, Stony Brook, New York 11794, USA

[c] Department of Biochemistry and Molecular Pharmacology, University of Massachusetts Medical School, Worcester, Massachusetts 01605, USA

[d] Graduate Program in Biochemistry & Structural Biology, Stony Brook University, Stony Brook, New York 11794, USA

*Corresponding Author: daniel.raleigh@stonybrook.edu; Tel 631 632 9547

ABBREVIATIONS: M_{Se}, selenomethionine; M_{SeO}, selenomethionine selenoxide; M_{ox}, methionine sulfoxide; F_{CN}, *p*-cyanophenylalanine; CTL9, C-terminal domain of ribosomal protein L9; HP36, 36 residue fragment of the villin headpiece helical subdomain; TFA, trifluoroacetic acid; MALDI-TOFMS, matrix-assisted laser desorption/ionization time-of-flight mass spectrometry; LC-ESI-TOFMS, liquid chromatography electrospray ionization time-of-flight mass spectrometry; CD, circular dichroism spectroscopy; MEM, maximum entropy model; MD, molecular dynamics; SASA, solvent-accessible surface area.

ABSTRACT Fluorescence spectroscopy, relying on intrinsic protein fluorophores, is one of the most widely used methods for studying protein folding, protein-ligand interactions, and protein dynamics. Tryptophan is usually the fluorophore of choice, given its sensitivity to environment and having the highest quantum yield of the natural amino acids, however changes in tryptophan florescence can be difficult to interpret in terms of specific structural changes. The introduction of quenchers of tryptophan fluorescence can provide information about specific structures, particularly if quenching is short range, however the most commonly employed quencher is histidine, and it is only effective when the imidazole sidechain is protonated, thus limiting the pH range over which this approach can be employed. In addition, histidine is not always a conservative substitution and is likely to be destabilizing if inserted into the hydrophobic core of proteins. Here we illustrate the use of a Trp-selenomethionine (M_{Se}) pair as a specific probe of protein structure. M_{Se} requires close approach to Trp to quench its fluorescence, and this effect can be exploited to design specific probes of α-helix and β-sheet formation. The approach is illustrated using equilibrium and time-resolved fluorescence measurements on designed peptides and globular proteins. M_{Se} is easily incorporated into proteins, provides a conservative replacement for hydrophobic sidechains, and M_{Se} quenching of Trp fluorescence is pH independent. The oxidized form of $M_{Se,}$ selenomethionine selenoxide, is also an efficient quencher of Trp fluorescence.

KEYWORDS: Selenomethionine, Tryptophan Fluorescence, Fluorescence Quenching, Protein Structure, Protein Folding

Fluorescence spectroscopy is one of the most accessible and widely used methods for studies of proteins. High sensitivity and time resolution make fluorescence methods attractive for studies of protein structure, dynamics, stability and aggregation.[1, 2] Naturally occurring tryptophan residues offer the simplest sensitive, non-perturbative intrinsic fluorophore. In addition to a shift in emission maximum upon exclusion from solvent, Trp undergoes changes in quantum yield, although the molecular basis of these changes can be difficult to interpret as they are determined by a number of factors. One approach towards simplifying Trp fluorescence experiments is introduction of a quencher.[3] Of the naturally occurring amino acids, His is probably the most commonly employed potent quencher of Trp fluorescence. However, the quenching mechanism of the Trp-His pair requires a protonated imidazole ring, restricting the utility of this system to pH ranges below the pK_a of His. Incorporation of a His residue in the interior of a protein can also be destabilizing, especially if it is protonated. A growing body of work has made use of the unnatural amino acid *p*-cyanophenylalanine (F_{CN}), the cyano analogue of Tyr, as an alternative to Trp.[4-9] His can also be used to quench F_{CN} fluorescence, but in this case is only effective above the pK_a of the imidazole ring, unlike in the Trp-His pair.[10]

Selenomethionine (M_{Se}), the selenium analogue of Met, is an effective pH independent quencher of F_{CN} fluorescence, and earlier work suggests that it may also quench Trp fluorescence.[11-14] The F_{CN} quenching effect occurs through an electron transfer mechanism which requires van der Waals contact between the side chains, making the approach complementary to related methods such as Förster Resonance Energy Transfer (FRET) which can be used to probe the distance between two fluorophores, but cannot definitively confirm whether they are in direct contact.[11, 15]

Although the F_{CN}-M_{Se} pair is a useful probe of structure, incorporation of the pair into an expressed protein does present some technical challenges. Methods for the incorporation of F_{CN}

using so-called 21st pair technology through the use of an unnatural aminoacyl-tRNA synthetase/tRNA pair have been developed.[7, 8] There is an extensive body of work on the incorporation of M_{Se} in high yield by Met auxotrophic cell lines for multi-wavelength anomalous diffraction (MAD) phasing in X-ray crystallography and ^{77}Se NMR.[16, 17] Simultaneous incorporation of both unnatural amino acids into a single protein has not yet been demonstrated but is possible, however it could result in low protein yields and could present a significant challenge. A more straightforward approach is to exploit the natural fluorophore Trp and to use well documented methods for the incorporation of M_{Se}. The unbranched alkyl side chain of M_{Se} is likely to be less perturbative at many sites in a protein than the polar aromatic ring of His, suggesting that Trp-M_{Se} pairs could provide a widely applicable protein of protein structure.

Here we demonstrate the use of M_{Se} quenching of Trp fluorescence to probe protein structure and to monitor protein unfolding. The fluorophore-quencher pair is incorporated recombinantly into a β-sheet in the C-terminal domain of ribosomal protein L9 (CTL9). The Trp-M_{Se} pair is also studied in two α-helical systems: a synthetic designed 21-residue helical peptide and a 36-residue segment of the villin headpiece helical subdomain (HP36). The results indicate that Trp-M_{Se} pairs can be used to probe local conformational changes, including the formation of specific α-helices and β-sheets at both high and low pH. The single oxidation product of M_{Se}, selenomethionine selenoxide (M_{SeO}), is also shown to be an effective quencher of Trp fluorescence.

MATERIALS AND METHODS

Peptide Synthesis

The 21-residue helical peptide and HP36 were synthesized using standard 9-fluorenylmethyloxycarbonyl (Fmoc) chemistry on a CEM Liberty microwave peptide synthesizer. Use of 5-(4'-Fmoc-aminomethyl-3',5-dimethoxyphenol)valeric acid (Fmoc-PAL-PEG-PS) resin

afforded an amidated C-terminus on both peptides, and acetic anhydride was used to acetylate the N-terminus of the helical peptide. β-branched residues, prolines, arginines and the C-terminal residue were double coupled. Peptides were deprotected and cleaved from resin in trifluoroacetic acid (TFA) with 5% thioanisole, 3.3% anisole and 3% 1,2-ethanedithiol as scavengers. Resin was removed by filtration and isolated peptides were precipitated in cold diethyl ether and pelleted by centrifugation at 10,000 rcf for 10 min. The supernatant was discarded; peptides were solubilized in 20% acetic acid and lyophilized.

Protein Expression

Mutants of CTL9 containing M_{Se} were expressed in M15MA *E.coli* cells carrying the CTL9 gene on a pQE-80L vector. A pREP4 plasmid was also present to repress "leaky" expression before induction. CTL9 mutants containing M_{Se} were expressed in M9 minimal media. An overnight culture of M15MA-pQE-80L-Y126W/H144M_{Se}-CTL9 was grown in LB rich media treated with ampicillin (200 μg/mL) and kanamycin (35 μg/mL) and added to 0.5 L of M9 minimal media supplemented with the 20 natural amino acids (40 mg/L) and treated with ampicillin (200 μg/mL) and kanamycin (35 μg/mL). Cells were grown at 37 °C to an optical density at 600 nm of 0.8-1, harvested by centrifugation at 5,000 rcf for 15 min and resuspended in 0.5 L of fresh M9 buffer solution treated with antibiotics. Cells were harvested a second time by centrifugation at 5,000 rcf for 15 min, resuspended in 0.5 L of fresh M9 minimal media supplemented with 19 of the natural amino acids (except methionine) and grown at 37 °C for 20 min. M_{Se} (40 mg/L) was added to the media, cells were grown at 37 °C for an additional 20 min and protein expression was induced by addition of isopropyl β-D-1-thiogalactopyranoside (IPTG) to a final concentration of 1 mM. After 4 hr cells were harvested by centrifugation at 5,000 rcf for 15 min. CTL9 mutants without M_{Se} were expressed in LB rich media using standard methods.

Protein and Peptide Purification

Harvested cells were lysed by sonication and protein partially purified from the cell lysate by cation exchange chromatography on a GE Sepharose Fast Flow column. Proteins were purified from the eluate by reversed-phase high performance liquid chromatography (HPLC) on a Higgins Analytical Proto 300 C18 preparative column. Synthetic peptides were purified by HPLC using the same column. A two-buffer A-B gradient system was used where buffer A was 0.1% (v/v) TFA in water and buffer B was 0.1% (v/v) TFA in 9:1 acetonitrile:water. All peptides and proteins were eluted with a linear gradient of 20-60% B in 40 min.

Protein Oxidation

Purified proteins were dissolved in 18 MΩ H_2O to a concentration of 1 mg/mL. The solution was acidified by addition of $HClO_4$ to a final concentration of 0.2 mM. Oxidation was initiated by addition of H_2O_2 to a final concentration of 0.005%. Trial experiments, monitored by HPLC indicated that 4 hours was an optimal incubation time for this system to maximize the production of the single oxidation product, selenomethionine selenoxide. Thus the reaction was allowed to proceed for 4 hr before dilution with 0.1% TFA in H_2O and the oxidized protein was purified by HPLC.

Mass Spectrometry

Peptides and proteins were characterized by matrix-assisted laser desorption/ionization time-of-flight mass spectrometry (MALDI-TOFMS) on a Bruker Daltonics autoflex TOF/TOF instrument. 21-residue helical peptide expected mass: 2014.987 Da (mono) observed: 2015.687 Da (mono). N68M_{Se}-HP36 expected mass: 4252.141 Da (mono) observed: 4252.315 Da (mono). N68M-HP36 expected mass: 4204.197 Da (mono) observed: 4207.8 Da (mono). Y126W-CTL9 expected mass: 10004.51 Da (average) observed: 10000.5 Da (average). Y126W/H144M_{Se}-CTL9 expected mass:

10045.46 Da (average) observed: 10045.509 Da (average). Y126W/H144M-CTL9 expected mass: 9998.55 Da (average) observed: 9998.3 Da (average).

Oxidized proteins were characterized by liquid chromatography electrospray ionization time-of-flight mass spectrometry (LC-ESI-TOFMS) on an Agilent G6224a oaTOF instrument. Oxidation products purified by HPLC were further separated on a Jupiter C18-MW-22.m column by a sequence of increasingly steep linear gradients from 0.1% acetic acid in water to 0.1% acetic acid in 9:1 acetonitrile:isopropanol and ionized by electrospray ionization (ESI). Y126W/H144M-CTL9 expected mass: 9998.69 Da (average) observed: 9999.09 Da (average). Y126W/H144M_{ox}-CTL9 expected mass: 10014.69 Da (average) observed: 10014.99 Da (average). Y126W/H144M_{Se}-CTL9 expected mass: 10045.46 Da (average) observed: 10046.01 Da (average). Y126W/H144M_{SeO}-CTL9 expected mass: 10061.46 Da (average) observed: 10062.00 Da (average).

Circular Dichroism Spectroscopy

Circular dichroism (CD) measurements were performed on an Applied Photophysics Chirascan spectrometer. CD wavelength scans were recorded in a 1 mm pathlength quartz cuvette with a thermostated sample holder at 20 °C from 190 to 260 nm in buffer and from 210 to 260 nm in urea using a 1 nm stepsize. Spectra were recorded as the average of three scans with an averaging time of 0.5 s.

Equilibrium Fluorescence

Fluorescence emission spectra were recorded on a Photon Technologies International fluorimeter in a 10 mm x 10 mm quartz cuvette using a slit width of 0.8 mm. Using an excitation wavelength of 280 nm, spectra were recorded from 290 to 450 nm with a step size of 1 nm and an averaging time of 1 s.

Time-resolved Fluorescence

Time-resolved fluorescence experiments were performed at the University of Massachusetts Medical School in Worcester, MA. Decays were measured on a home-built time correlated single photon counting (TCSPC) apparatus. The tripled output of a 10 W Verdi (Coherent) pumped Ti:sapphire laser (Coherent Mira) was used to excite Trp at 292 nm. The repetition rate was reduced to 3.8 MHz. The detection utilized a bandpass filter (FF01-357/44, Semrock, Rochester, NY) and Glan-Taylor polarizer at the magic angle. A PMH-100-6 photomultiplier tube connected to an SPC150 photon counting card (Becker-Hickl, Berlin, Germany) was used for TCSPC. The instrument response was collected using scattered light from a solution of distilled deionized water using a bandpass filter that partially overlaps the excitation wavelength. The peak counts in the instrument response were approximately 30,000 counts. The instrument response exhibits a full width at half-maximum of approximately 200 ps and is primarily determined by the response of the photomultiplier tube. All measurements were collected at 20 ±1 °C. The decay curves were fit using a maximum entropy model (MEM) with reconvolution of the instrument response.[18]

Molecular Dynamics Simulations

The starting structures for HP36 and CTL9 were constructed using the pdb files 1YRF[19] (Chiu *et al*. incorporated an N68H mutation as a fluorescence quencher) and 1DIV[20], respectively. For A single Met residue was added to the N-terminus of the structure of HP35 (PDB: 1YRF) to generate HP36, and the mutation H68M-HP36 was made by using Swiss PDB.[21] The PDB file 1DIV is for full length L9 and residues 1 to 57 were deleted to generate CTL9. Tyr 126 was changed to Trp and His 144 was changed to Met. These modified structures were equilibrated by molecular dynamics (MD) simulations with restraints on unmodified residues. Simulations were performed using the Amber software package with the Amber ff14SB force field and TIP3P

water.[22, 23] The step size was set to 2 fs. Truncated octahedron boxes with periodic boundary condition were used. The cutoff of non-bonded interactions was set to 8 Å. No ions were included in the simulation. Particle mesh Ewald methods were used to evaluate electrostatic energies.[24] Hydrogen atoms were constrained using the SHAKE algorithm.[25] The temperature was set to 298 K by using a weak-coupling algorithm with the coupling constant set to 1 ps.[26] A constant pressure of 101,325 pascal controlled by the Berendsen barostat was used.[26] The program Cpptraj was used to calculate distances, dihedral angles and the solvent accessible surface area (SASA).[27]

RESULTS AND DISCUSSION

Tryptophan Selenomethionine Pairs Provide a Fluorescence Probe of β-sheet Formation

Trp and M_{Se} residues were recombinantly incorporated into the C-terminal domain of ribosomal protein L9 (CTL9) in order to examine the utility of the Trp-M_{Se} pair to monitor folding in globular proteins. The N-terminal M_{Se} residue is efficiently cleaved and no product with an additional M_{Se} residue was observed based on MALDI-TOFMS data. The numbering system used here is based upon full length L9 and designates the first residue in CTL9 as residue 58. This 92 residue, mixed α-β protein possesses naturally occurring Tyr and His residues at positions 126 and 144 on the second and third β-strands, respectively. The residues are located in an antiparallel β-sheet with the side chains in van der Waals contact. Three mutants were prepared, one with Tyr 126 mutated to Trp (Y126W-CTL9), another with Tyr 126 and His 144 mutated to Trp and M_{Se}, respectively (Y126W/H144M_{Se}-CTL9), and a third with Tyr 126 and His 144 mutated to Trp and Met, respectively (Y126W/H144M-CTL9) (Figure 1A). Circular dichroism (CD) confirmed that all mutants are folded in buffer and fully unfolded in buffer with 9.5 M urea (Supporting Information Figure S1).

Trp fluorescence is high in the unfolded state at pH 7.5 (20 mM tris, 9.5 M urea) for Y126W/H144M$_{Se}$-CTL9, and 66% quenched in the folded state (Figure 1B). In contrast, the fluorescence intensity of Y126W-CTL9 and Y126W/H144M-CTL9 is higher in the folded state than in the urea unfolded state (9.5 M urea) at pH 7.5 (Figure 1C, D). This effect is likely due to partial burial of Trp 126 in the native state. The solvent accessible surface area (SASA) of Trp 126 in the folded state of Y126W/H144M-CTL9 calculated using trajectories obtained from MD simulations is 106.0 Å^2. The SASA of Trp in a reference state corresponding to a fully extended penta-peptide with the sequence from CTL9 (Leu-Gly-Trp-Thr-Asn) is 144.0 Å^2. Histidine is known to be a quencher of Trp fluorescence, however the quenching mechanism requires the imidazole ring to be in the protonated state. As expected, significantly enhanced quenching—90% relative to the unfolded state—is observed for Y126W-CTL9 at pH 5.0 where His 144 is protonated (Supporting Information Figure S2A). In contrast, no fluorescence quenching was observed for Y126W/H144M-CTL9 at pH 7.5 or 5.0 (Supporting Information Figure S2E, F). The pH dependent data illustrates the practical limitations of His as a quencher of Trp fluorescence. In contrast, Trp fluorescence was efficiently quenched by M$_{Se}$ at both pH values. The fluorescence quenching efficiency of M$_{Se}$ was 66% at pH 5.0 and 7.5 relative to the respective unfolded states (Supporting Information Figure S2C, D). The pH dependent studies illustrate the advantage of Trp-M$_{Se}$ over Trp-His pairs, namely that quenching is pH independent which in turn makes the interpretation of the data more straightforward.

The dynamic quenching effects in Y126W/H144M$_{Se}$-CTL9 were examined by conducting fluorescence lifetime measurements in 20 mM tris buffer at pH 7.5 and in the presence of 9.5 M urea under the same conditions (Figure 2). Maximum entropy model (MEM) analysis of the data indicates a single lifetime distribution centered around 3 ns in the urea unfolded state and two

lifetime distributions centered around and 3 ns and 0.1 ns in the folded state. The two lifetime distributions have similar intensities in the folded state, though the intensity of the 0.1 ns lifetime distribution is slightly higher. Based on the known stability of CTL9, the 3 ns lifetime distribution in the folded state cannot represent unfolded protein; the population of folded molecules is estimated to be in excess of 99.4% under these conditions. Instead this population likely represents rotameric states of Trp which are not within van der Waals contact of the Se atom and therefore do not experience quenching. The existence of such states is supported by modeling of the different rotameric states of Trp (Supporting Information Figure S3).

Long time MD simulations of Y126W/H144M-CTL9 were conducted to test this hypothesis. Since M_{Se} is not parametrized in the Amber force field, Met was used in the simulations. A total of four independent simulations were carried out. In the first and second runs, W126 starts in the rotamer state of χ_1 = -65.0°, χ_2 = -84.9°, which is the rotamer state found in the crystal structure (1DIV). The third run starts with a rotamer state of χ_1 = -71.2°, χ_2 = 94.3°, and the fourth run starts with a rotamer state of χ_1 = 62.1°, χ_2 = 94.4°. The distances between W126 and M144 were measured using the geometric center of Cδ2 and Cε2 of W126, and the sulfur atom of Met for each frame of the simulations (Supporting Information Figure S4). The χ_1 and χ_2 dihedral angles were calculated for the first run (Supporting Information Figure S5) and show a clear correlation between the rotameric state of W126 and the distance between W126 and M144 (Supporting Information Figure S4A). Three clusters of distances, which are centered around 4 Å, 5 Å and 7 Å are observed when the distances between W126 and M144 from all four MD simulations are plotted as a histogram (Supporting Information Figure S6). Over the course of a 3 ns simulation with a sampling frequency of 0.002 ns, the distances jumped multiple times between 4 Å and 5 Å (Supporting Information Figure S7) which indicates that distances at 4 Å and 5 Å are in rapid

exchange; this likely accounts for the experimental lifetime distribution centered around 0.1 ns. The longer lifetime of 3 ns likely corresponds to a distance of 7 Å between W126 and M_{Se}144. The absence of a short lifetime distribution for CTL9 in the presence of 9.5 M urea indicates that Trp does not experience significant quenching under these conditions as the β-sheet is not formed.

Oxidation of Selenomethionine to the Selenoxide Does Not Abolish Quenching

Selenium is more susceptible to oxidation than sulfur, but it is not immediately clear what effect this will have on the quenching efficiency of M_{Se}. Selenomethionine, like methionine, can undergo oxidation to selenomethionine selenoxide (M_{SeO}) and further oxidation to selenomethionine selenone (Figure 3A). No spontaneous oxidation of Y126W/H144M_{Se}-CTL9 was detected by ESI LC-MS following protein expression and purification. To examine the differences in oxidation susceptibility between Met and M_{Se}, Y126W/H144M-CTL9 and Y126W/H144M_{Se}-CTL9 were exposed to oxidizing conditions. Exposure to 0.005% H_2O_2 acidified with 0.2 mM $HClO_4$ for 4 hours was found to oxidize ~90% of Y126W/H144M_{Se}-CTL9 to Y126W/H144M_{SeO}-CTL9, while only oxidizing ~10% of Y126W/H144M-CTL9 based on HPLC monitored by UV absorbance at 220 nm (Supporting Information Figure S8). Analysis by LC-ESI-TOFMS found no evidence of oxidation of either protein to the selenone or sulfone. CD confirmed that Y126W/H144M_{SeO}-CTL9 was properly folded in buffer and fully unfolded in buffer with 9.5 M urea (Figure 3B).

After correcting for concentration, the Trp fluorescence of Y126W/H144M_{SeO}-CTL9 was identical to that of Y126W/H144M_{Se}-CTL9 in 9.5 M urea, 20 mM tris buffer at pH 7.4. The quenching efficiency of Y126W/H144M_{SeO}-CTL9 upon folding in 20 mM tris buffer at pH 7.4 was 84%, compared to 66% for Y126W/H144M_{Se}-CTL9 under the same conditions (Figure 3C, D). The only moderately higher susceptibility of M_{Se} to oxidation compared to Met, together with the modest differences in quenching efficiency of M_{Se} *vs* M_{SeO} indicate that oxidation is unlikely

to be a significant source of error in applications of M_{Se} as a fluorescence quencher, provided oxidation of M_{Se} does not perturb the structure of the protein

Tryptophan Selenomethionine Pairs Can be Used to Follow α-helix Formation in Globular Proteins

To investigate the utility of the Trp-M_{Se} pair as a probe of local α-helical structure in globular proteins, a mutant of the 36-residue villin headpiece helical subdomain (HP36) was prepared. HP36 is a small, autonomously folding three-helix protein that has been used widely as a model system for both computational and experimental studies of protein folding.[19, 28-39] HP36 possesses a naturally occurring Trp residue at position 24. We mutated Asn 28 to M_{Se} to create an *i*, *i*+4 arrangement that places the side chains roughly one turn apart, bringing them into close contact in the helical state. Thus we expect Trp fluorescence to be higher when the peptide is unfolded and lower when it adopts a helical conformation and is quenched by M_{Se} (Figure 4A). HP36 is a subdomain of villin, but the numbering system used here designates the first residue of HP36 as residue 1. This construct was designated N28M_{Se}-HP36. CD experiments in native buffer (20 mM acetate at pH 5.0) show that the substitution, as expected, does not perturb the secondary structure. The experimental CD spectrum is very similar to that of wild type HP36 reported in the literature.[32] The spectrum observed for N28M_{Se}-HP36 in buffer with 9.5 M urea indicates that the protein is fully unfolded under these conditions (Figure 4B).

The Trp quenching efficiency of M_{Se} in HP36 was first examined by comparing the equilibrium fluorescence intensity of folded N28M_{Se}-HP36 in 20 mM acetate buffer at pH 5.0 to the fluorescence intensity of the unfolded protein in buffer with 9.5 M urea (Figure 4C). Trp fluorescence is 60% quenched in the folded state relative to the unfolded state. Surprisingly, the quenching efficiency of N28M-HP36 was very similar (Figure 4D). The data indicates that, in this

system, M_{Se} offers little improvement over Met. Possible explanations include a closer approach of the Met side chain, which is not considered likely, or quenching of Trp fluorescence by other groups in both proteins. There are a number of Lys residues, K25, K30 and K31 near W24 in the primary sequence. MD simulations indicate that the epsilon amino group of K25 makes a close approach to the indole ring of W24; the mean distance from the nitrogen of the K25 sidechain to the geometric center of Cδ2 and Cε2 of the Trp is 6.9 ±1.1 Å during the simulation (Supporting Information Figure S9), which is expected to contribute to the quenching of Trp fluorescence. This case highlights the importance of choosing alternative fluorophores, such as 4-cyanophenylalanine, which is not quenched by Lys in the same manner as Trp. N28M_{Se}-HP36 appears to experience greater fluorescence quenching in the unfolded state than N28M-HP36 (Figure 4C, D). This might arise from non-helical interactions of the M_{Se} and Trp residues due to their proximity in primary sequence, transient helical structure even in the presence of urea, or some combination of these effects. Such interactions should also be present in the unfolded state of N28M-HP36 and the difference in quenching between the two proteins could be due to more effective quenching by M_{Se} or by small changes in the unfolded ensemble.

The dynamic quenching effects of M_{Se} on Trp in HP36 were examined by conducting fluorescence lifetime measurements in 20 mM acetate buffer at pH 5.0 and in the presence of 9.5 M urea in the same buffer (Figure 5). MEM analysis of the data indicates two lifetime distributions centered around 4 ns and 1 ns in both the folded state and the urea unfolded state. The 4 ns lifetime distribution is the major component of the decay in the urea unfolded state while the 1 ns lifetime distribution is the major component in the folded state.

The presence of a short lifetime component in the urea unfolded state supports the conclusion from the equilibrium fluorescence data that the Trp residue still experiences some quenching under

these conditions. The presence of a long lifetime component in the absence of urea could arise from contributions from a small unfolded population or rotameric states of the Trp sidechain that are not within van der Waals contact with the Se atom even in the helical conformation. Based on the known stability of HP36, the small, long-lifetime population in the absence of urea most likely represents an unquenched rotameric state of Trp rather than a non-helical population (Supporting Information Figure S10).

Tryptophan Fluorescence Quenching by Selenomethionine Probes α-helix Formation in a Designed Peptide

We next tested the utility of the approach using a designed 21-residue helical peptide (Figure 6A). The studies with the peptide also provide additional clues as to the origin of the short and long lifetime components. The synthetic peptide included Ala residues to induce helical structure, Lys residues to improve solubility, and an Asp-Pro pair at the N-terminus that acts as an initiator of helical structure. The N and C-termini were acetylated and amidated, respectively, to increase the stability of the helical state. A Trp residue was incorporated at position 12 and M_{Se} at position 16 to produce the same *i*, *i*+4 configuration used in HP36 (Figure 6A). Helical structure was confirmed by CD (Figure 6B). Data indicates significant helical structure in 10 mM acetate buffer at pH 5.5, indicated by a local minimum at 222 nm and a maximum at 193 nm. The helical content of the peptide in buffer was estimated to be 38% based on the molar ellipticity at 222 nm (Supporting Information Equation S1). In contrast, the spectrum observed in the same buffer with 8 M urea indicates that the peptide is unstructured under these conditions. The ability of M_{Se} to quench Trp fluorescence was examined by comparing the fluorescence intensity of the peptide in buffer and in the presence of denaturant. Fluorescence is high in the unfolded state (8 M urea) and is 35% quenched under folding conditions (10 mM acetate buffer at pH 5.5) (Figure 6C). The

smaller magnitude of the effect compared to the 60% quenching efficiency observed for N28M$_{Se}$-HP36 can be attributed to the fact that the peptide is not fully folded in the absence of urea while N28M$_{Se}$-HP36 is. Consequently, the quenching observed for the 21-residue helical peptide represents Trp quenching in only a fraction of molecules in the sample whereas nearly all Trp residues are quenched in a sample of N28M$_{Se}$-HP36 under folding conditions.

The effect of M$_{Se}$ quenching on the Trp fluorescence lifetime was examined by conducting fluorescence lifetime measurements in 10 mM acetate buffer at pH 5.5 and in the presence of 8.0 M urea under the same conditions (Figure 7). MEM analysis indicates the presence of two lifetime distributions centered around 3 ns and 1 ns in both the folded state and in the urea unfolded state. The lifetimes of the individual components are similar in urea and in buffer, but the relative intensities are not. Whereas the decay is dominated by the 3 ns lifetime distribution in the urea unfolded state, the 1 ns lifetime distribution is the major component in the folded state.

The results of the MEM analysis of the 21-residue helical protein are broadly similar to the results of the MEM analysis of N28M$_{Se}$-HP36. The most significant difference is that the relative intensity of the short lifetime distribution in the HP36 sample is higher in both the presence and absence of urea compared to the relative intensity of the short lifetime distribution in the helical peptide sample under the same conditions. This effect is more pronounced in the folded state than in the urea unfolded state. This suggests that conformations in which Trp fluorescence is quenched are more highly populated in N28M$_{Se}$-HP36 than in the helical peptide, which is consistent with CD data that indicates higher helicity in the folded state of HP36 than in the helical peptide, as well as equilibrium fluorescence data which shows a higher Trp quenching efficiency in N28M$_{Se}$-HP36 than in the helical peptide. The relative intensity of the short lifetime distribution is higher in buffer than what might be expected for a peptide which is only 38% helical based on the CD

data. However, CD is a global probe of structure and the effect could be due to higher local helicity in the vicinity of the Trp-M_{Se} pair, ie. the ends of the helix are frayed while the core of the helix is more structured.

CONCLUSIONS

The data presented here illustrates the utility of Trp-M_{Se} pairs as non-perturbing fluorescence probes of protein structure. Advantages of the approach include the ease of incorporation of M_{Se}, the conservative nature of the substitution of Leu, Ile, Met and Val by M_{Se}, the pH independence of the observed quenching and the short range nature of the quenching, which facilitates the interpretation of fluorescence changes in terms of specific structural changes, including local conformation differences in the folded state, as exemplified by the sensitivity of the lifetime distributions to the rotameric state of Trp 126 in CTL9. Potential issues include the fact that M_{Se} may not always be a conservative replacement for a surface residue owing to its hydrophobicity. Oxidation of M_{Se} to the selenoxide does not affect quenching, but the increased bulk caused by the additional oxygen atom could make the substitution less conservative in cases where packing is important. Trp-His pairs have been widely used as a fluorescence probe of protein structure and are complementary to the Trp-M_{Se} approach illustrated here. M_{Se} is a more conservative substitution in the hydrophobic core of a protein or in transmembrane helices than His. His on the other hand may be a more conservative replacement for surface exposed hydrophilic residues.

The lifetime of the slow component (~3-4 ns) is similar in all three systems investigated here, but the rapidly decaying component of the curve has a shorter lifetime in CTL9 (~0.1 ns) than in the other systems studied (~1 ns). This is consistent with the closer approach of Trp and M_{Se} in the folded state of Y126W/H144M_{Se}-CTL9 than in the helical peptide or N28M_{Se}-HP36. The positioning of the Trp-M_{Se} pair on the antiparallel β-sheet of CTL9 brings the indole ring of Trp

in much closer proximity to the Se atom of M_{Se} than does introducing the pair at *i* and *i*+4 positions in an α-helix, a conclusion supported by examining models of the low energy rotamers (Supporting Information Figure S11). This contrasts with the lifetime data in high urea for the helical peptide and N28M_{Se}-HP36, which indicates that Trp is at least partially quenched by M_{Se} even under denaturing conditions. The different effects observed in the urea unfolded states of the helical systems versus CTL9 are likely caused by transient contacts between the indole ring and Se atom in the helical systems, facilitated by their close proximity in primary sequence, in contrast the M_{Se} and Trp residues are further apart in primary sequence in CTL9. Low levels of residual helical structure could also contribute to the effects observed for the unfolded state of HP36.

The Trp-M_{Se} pair is complementary to the F_{CN}-M_{Se} pair.[11, 13] An advantage of F_{CN} is that it can be selectively excited against a background of Trp and Tyr residues, however incorporation of an F_{CN}-M_{Se} pair into an expressed protein does present more technical challenges than incorporation of a Trp-M_{Se} pair. Interesting future applications could include the incorporation of specific F_{CN}-M_{Se} and Trp-M_{Se} pairs into the same protein as orthogonal fluorescence probes of different structural elements.

In summary, the data presented here demonstrates the utility of Trp-M_{Se} pairs as a straightforward probe of specific elements of protein structure. The cases studied here involve monitoring α-helical and anti-parallel β-sheet structure, but the approach is not limited to these classes of secondary structure; any structure, including a parallel β-sheet or a loop which brings the two residues into van der Waals contact will lead to efficient quenching. The pair could also be used to monitor protein-ligand interactions provided complex formation leads to the close approach of the Se atom and the indole ring.

ASSOCIATED CONTENT

Supporting Information Available. Equations for the estimation of helical content, CD spectra, fluorescence emission spectra, side chain rotamer models, simulated side chain-side chain distance *vs* time plots, simulated side chain-side chain distance distributions, HPLC traces.

AUTHOR INFORMATION

Corresponding Author

*daniel.raleigh@stonybrook.edu; Tel 631 632 9547

Author Contributions

The manuscript was written through contributions of all authors. All authors have given approval to the final version of the manuscript. †These authors contributed equally.

Funding Sources

This work was supported by NSF MCB-1330259 grant to DPR and NIH GM23303 to OB. JZ was supported in part by a fellowship from the Laufer Center.

ACKNOWLEDGMENT

The authors thank Prof. Feng Gai for his encouragement and helpful discussions.

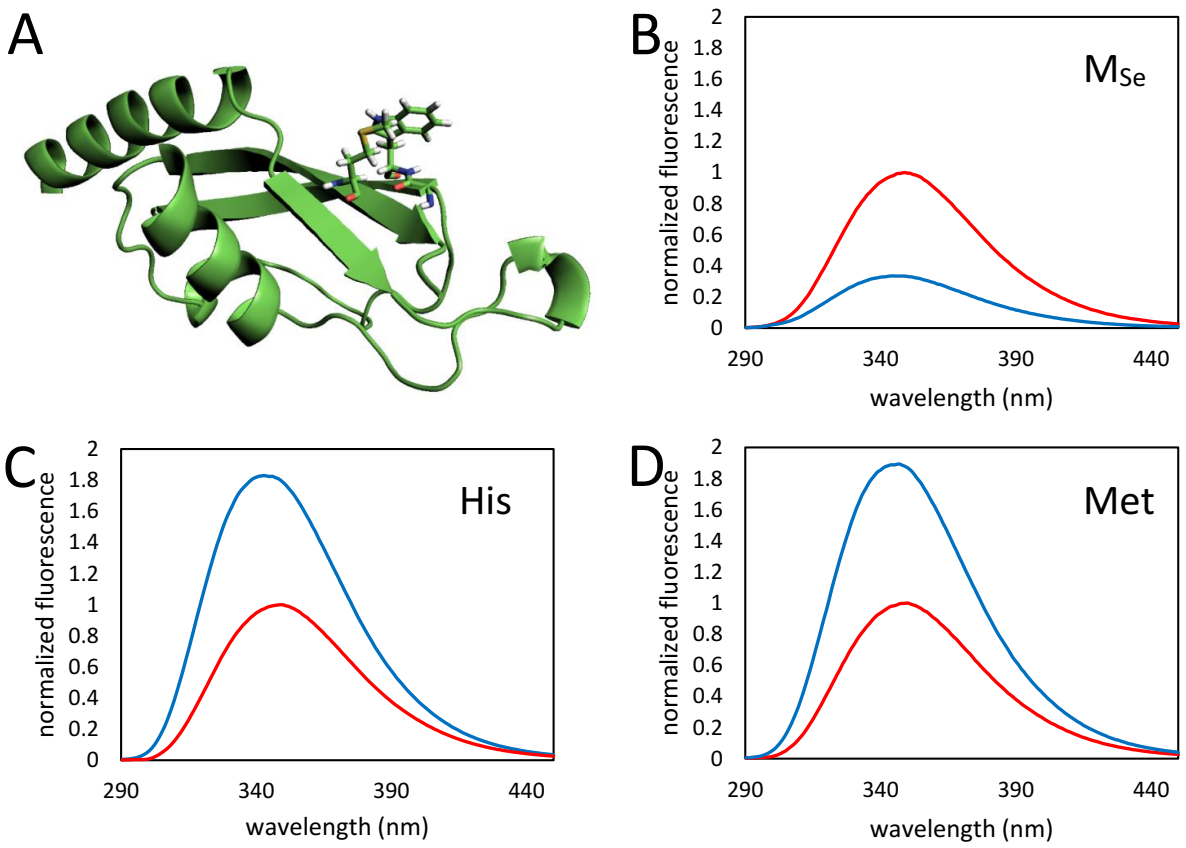

Figure 1: The fluorescence of Trp-M_{Se} pairs probe β-sheet formation. **(A)** Ribbon diagram of Y126W/H144M_{Se}-CTL9 based on PDB structure 1DIV showing the proximity of Trp and M_{Se} at positions 126 and 144.[20] **(B)** Fluorescence emission spectra of Y126W/H144M_{Se}-CTL9 at 20 °C in 20 mM tris buffer at pH 7.5 (blue) and in the same buffer with 9.5 M urea (red). **(C)** Fluorescence emission spectra of Y126W-CTL9 at 20 °C in 20 mM tris buffer at pH 7.5 (blue) and in the same buffer with 9.5 M urea (red). **(D)** Fluorescence emission spectra of Y126W/H144M-CTL9 at 20 °C in 20 mM tris buffer at pH 7.5 (blue) and in the same buffer with 9.5 M urea (red).

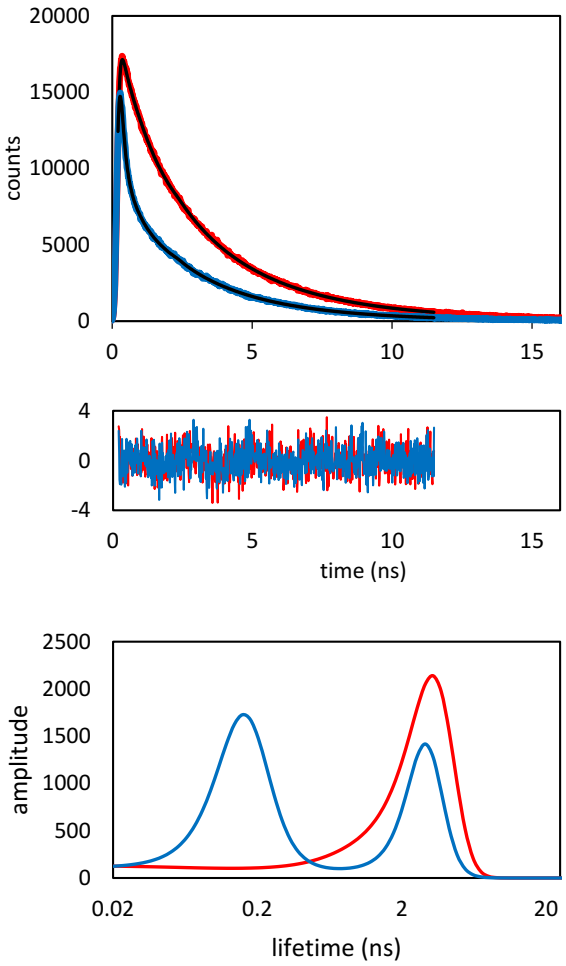

Figure 2: Maximum entropy analysis of time-resolved fluorescence decays of Y126W/H144M$_{Se}$-CTL9 in 20 mM tris buffer at pH 7.5 (blue) and in the same buffer with 9.5 M urea (red). Decays were fit using a maximum entropy model reconvoluted with the instrument response (black). Weighted residuals and the lifetime distributions are plotted below.

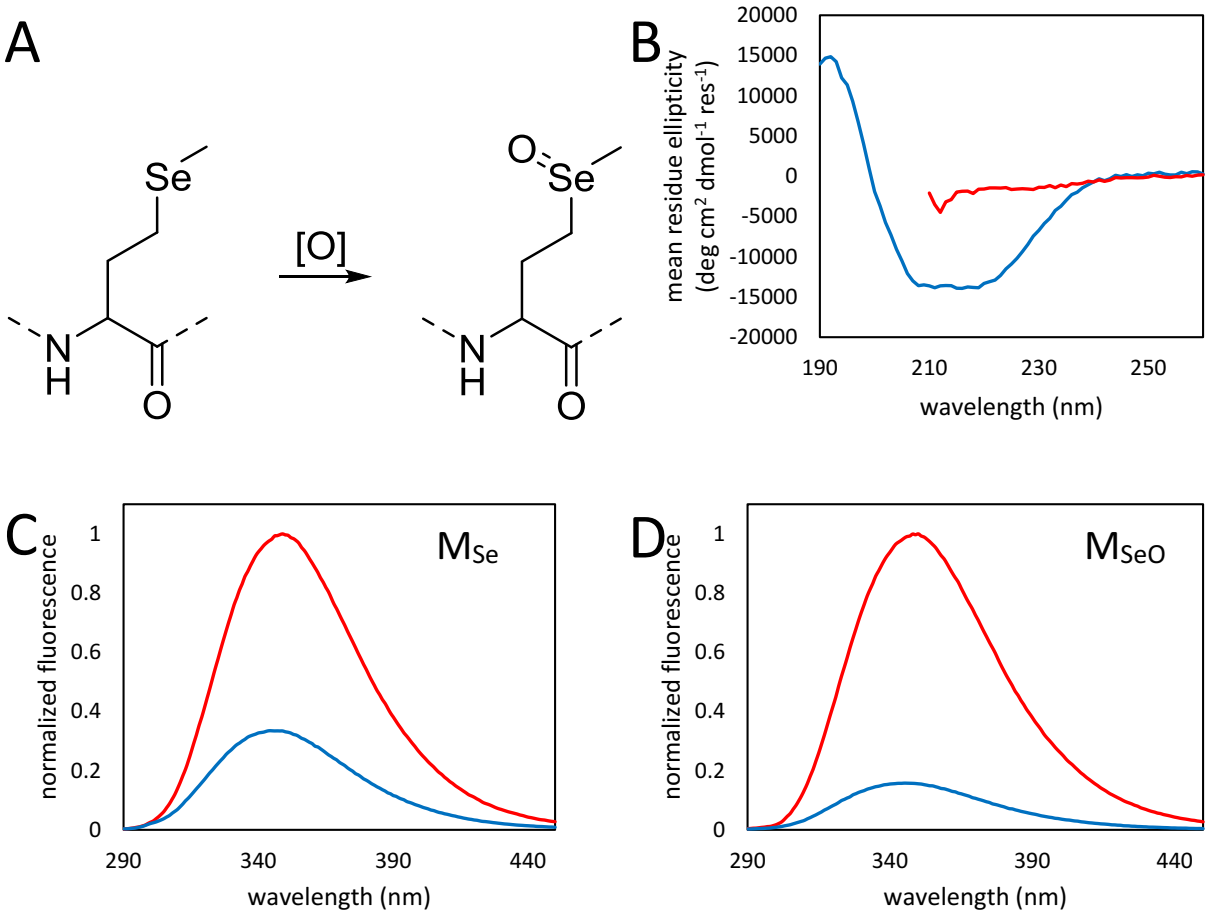

Figure 3. Oxidation of M_{Se} to M_{SeO} slightly increases fluorescence quenching efficiency. **(A)** Structure of selenomethionine (M_{Se}) and the oxidation product selenomethionine selenoxide (M_{SeO}). **(B)** CD spectra of Y126W/H144M_{SeO}-CTL9 at 20 °C in 20 mM tris buffer at pH 7.4 (blue) and in the same buffer with 9.5 M urea (red). **(C)** Fluorescence emission spectra of Y126W/H144M_{Se}-CTL9 at 20 °C in 20 mM tris buffer at pH 7.4 (blue) and in the same buffer with 9.5 M urea (red). **(D)** Fluorescence emission spectra of Y126W/H144M_{SeO}-CTL9 at 20 °C in 20 mM tris buffer at pH 7.4 (blue) and in the same buffer with 9.5 M urea (red). Note the decreased native state intensity for the selenoxide sample.

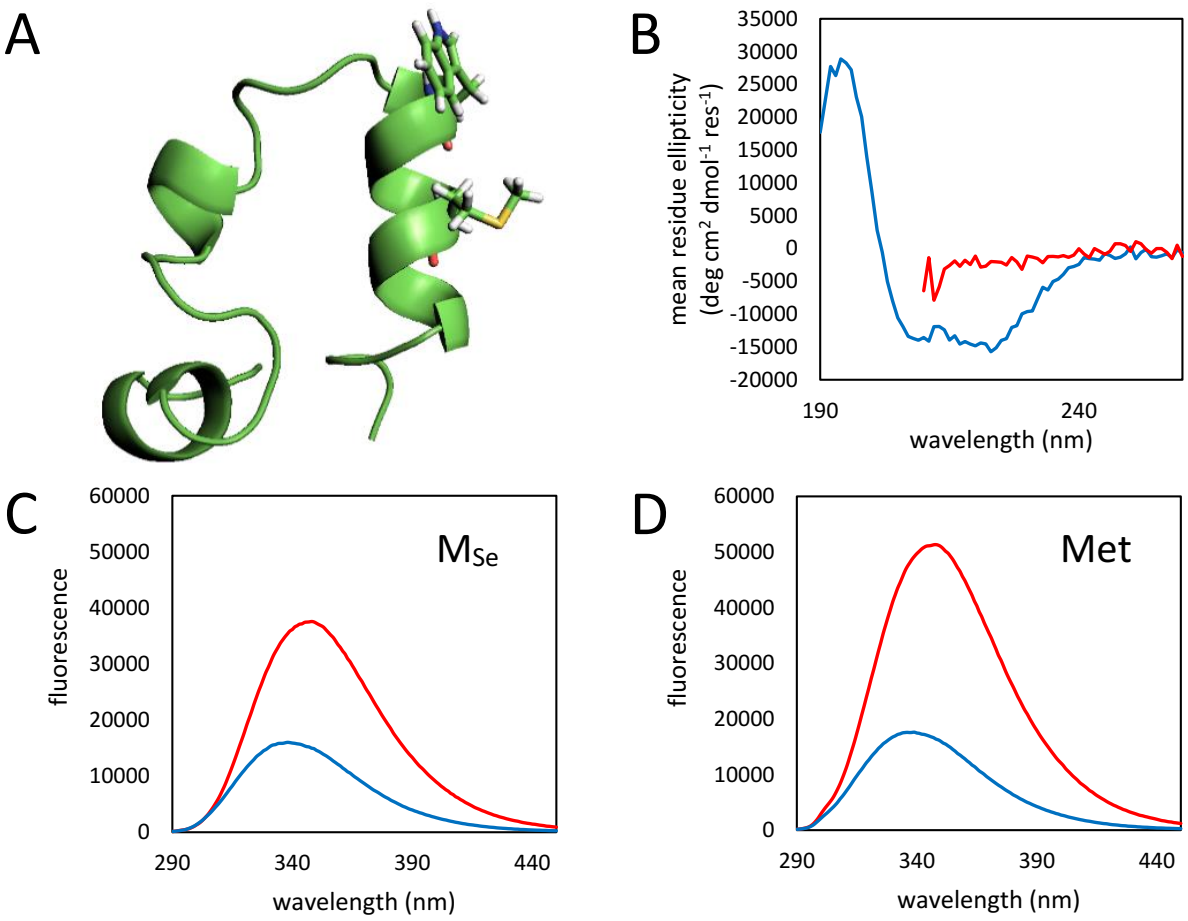

Figure 4: The fluorescence of Trp-M_{Se} pairs monitors the folding of helical proteins. **(A)** Ribbon diagram of HP36 based on PDB structure 1VII showing the proximity of Trp and M_{Se} at positions 24 and 28.[29] **(B)** CD spectra of N28M_{Se}-HP36 at 20 °C in 20 mM acetate buffer at pH 5.0 (blue) and in the same buffer with 9.5 M urea (red). **(C)** Fluorescence emission spectra of N28M_{Se}-HP36 at 20 °C in 20 mM acetate buffer at pH 5.0 (blue) and in the same buffer with 9.5 M urea (red). **(D)** Fluorescence emission spectra of N28M-HP36 at 20 °C in 20 mM acetate buffer at pH 5.0 (blue) and in the same buffer with 9.5 M urea (red).

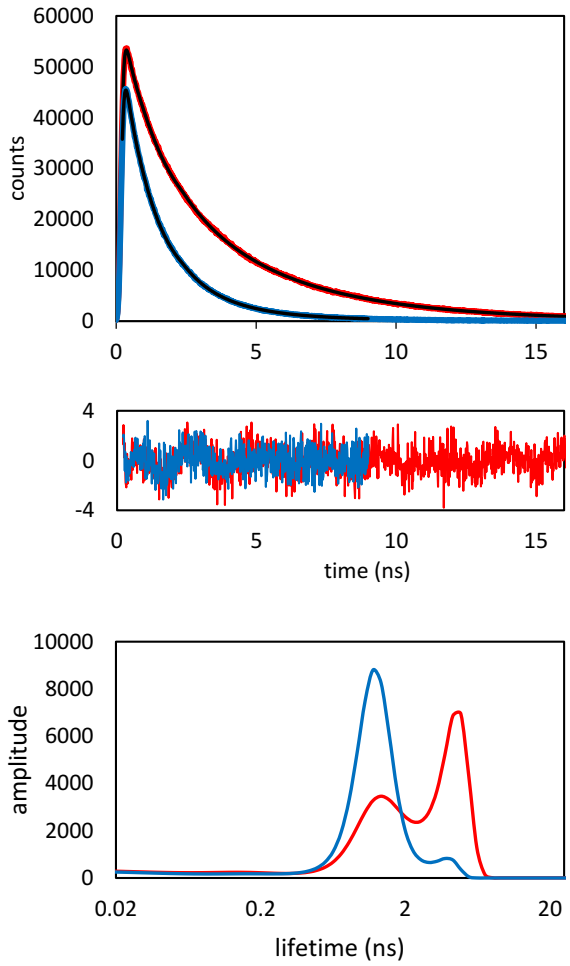

Figure 5: Maximum entropy analysis of time-resolved fluorescence decays of N28M$_{Se}$-HP36 in 20 mM acetate buffer at pH 5.0 (blue) and in the same buffer with 9.5 M urea (red). Decays were fit using a maximum entropy model reconvoluted with the instrument response (black). Weighted residuals and the lifetime distributions are plotted below.

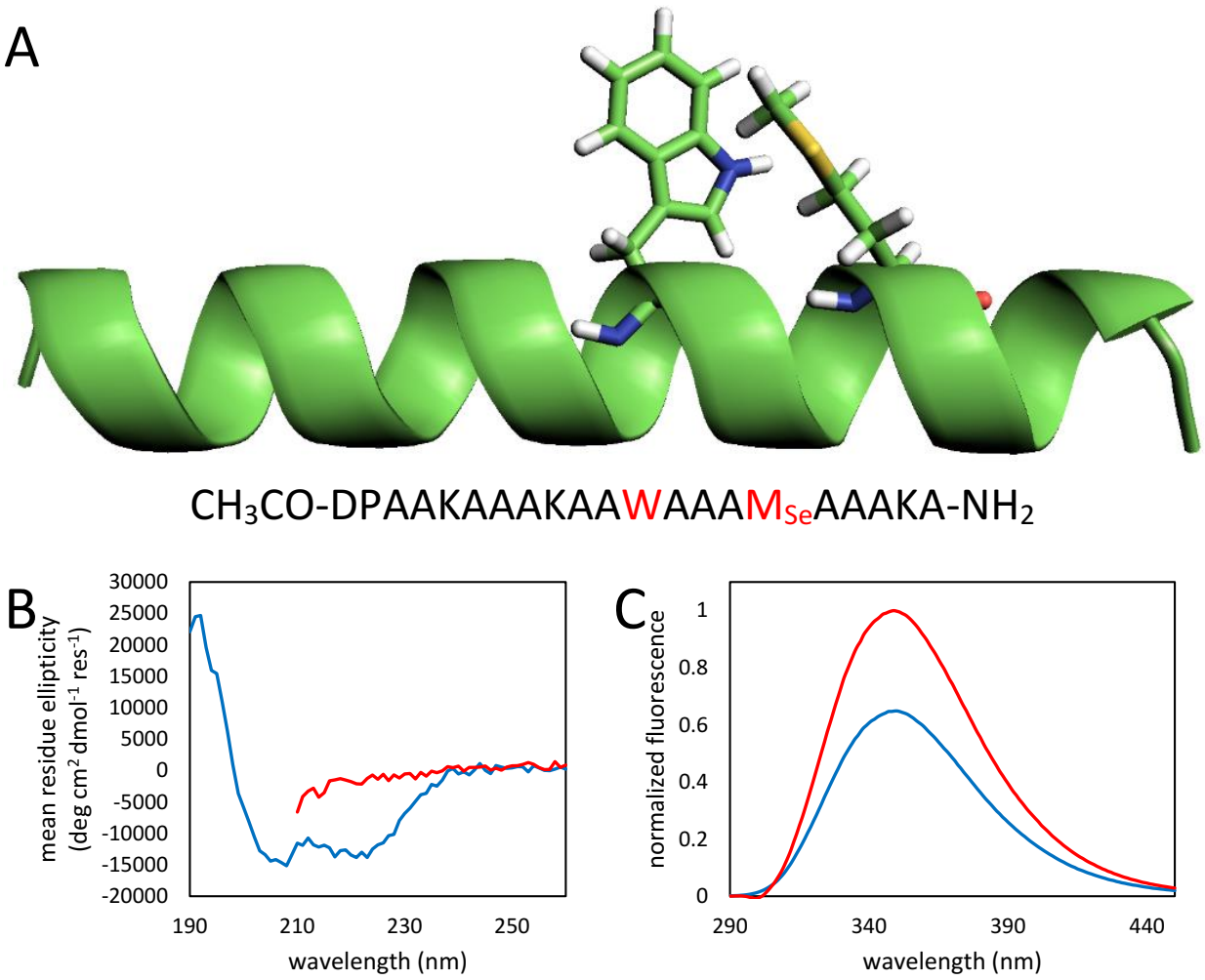

Figure 6: The fluorescence of Trp-M_{Se} pairs is sensitive to α-helix formation. **(A)** Sequence and ribbon diagram of an idealized 21-residue helical peptide showing the proximity of Trp and M_{Se} at positions *i* and *i*+4. **(B)** CD spectra of the 21-residue helical peptide at 25 °C in 10 mM acetate buffer at pH 5.5 (blue) and in the same buffer with 8.0 M urea (red). **(C)** Fluorescence emission spectra of the 21-residue helical peptide at 25 °C in 10 mM acetate buffer at pH 5.5 (blue) and in the same buffer with 8.0 M urea (red).

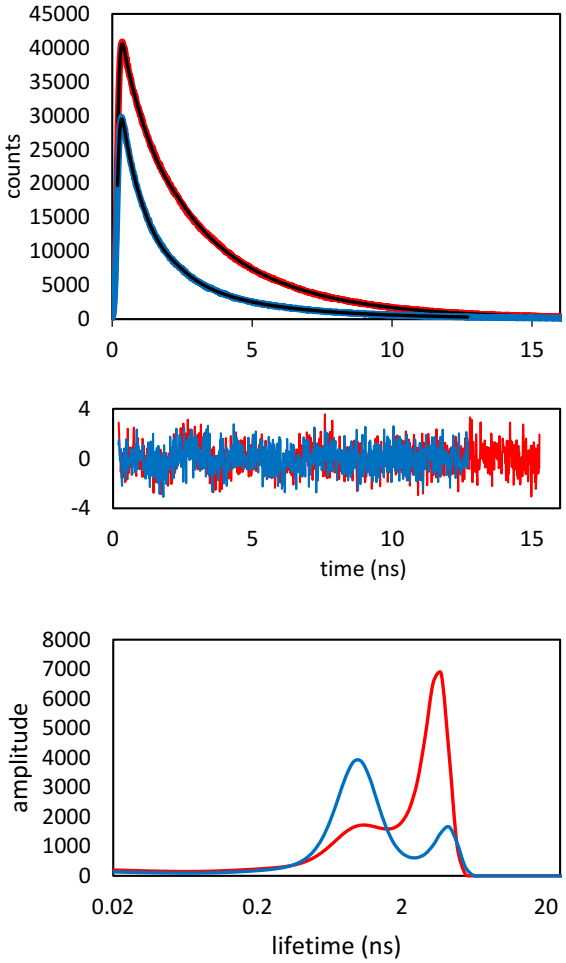

Figure 7: Time-resolved fluorescence decays of 21-residue helical peptide in 10 mM acetate buffer at pH 5.5 (blue) and in the same buffer with 8.0 M urea (red). Decays were fit using a maximum entropy model reconvoluted with the instrument response (black). Weighted residuals and the lifetime distributions are plotted below.

REFERENCES

[1] Lakowicz, J. R. (2006) *Principles of Fluorescence Spectroscopy*, 3 ed., Springer.

[2] Brown, M. P., and Royer, C. (1997) Fluorescence spectroscopy as a tool to investigate protein interactions, *Curr Opin Biotech 8*, 45-49.

[3] Kubelka, J., Eaton, W. A., and Hofrichter, J. (2003) Experimental tests of villin subdomain folding simulations, *J Mol Biol 329*, 625-630.

[4] Tucker, M. J., Oyola, R., and Gai, F. (2006) A novel fluorescent probe for protein binding and folding studies: p-cyano-phenylalanine, *Biopolymers 83*, 571-576.

[5] Tucker, M. J., Tang, J., and Gai, F. (2006) Probing the kinetics of membrane-mediated helix folding, *J Phys Chem B 110*, 8105-8109.

[6] Aprilakis, K. N., Taskent, H., and Raleigh, D. P. (2007) Use of the novel fluorescent amino acid p-cyanophenylalanine offers a direct probe of hydrophobic core formation during the folding of the N-terminal domain of the ribosomal protein L9 and provides evidence for two-state folding, *Biochemistry 46*, 12308-12313.

[7] Wang, L., Xie, J., and Schultz, P. G. (2006) Expanding the genetic code, *Annu Rev Biophys Biomol Struct 35*, 225-249.

[8] Miyake-Stoner, S. J., Miller, A. M., Hammill, J. T., Peeler, J. C., Hess, K. R., Mehl, R. A., and Brewer, S. H. (2009) Probing protein folding using site-specifically encoded unnatural amino acids as FRET donors with tryptophan, *Biochemistry 48*, 5953-5962.

[9] Rogers, J. M., Lippert, L. G., and Gai, F. (2010) Non-natural amino acid fluorophores for one- and two-step fluorescence resonance energy transfer applications, *Anal Biochem 399*, 182-189.

[10] Taskent-Sezgin, H., Marek, P., Thomas, R., Goldberg, D., Chung, J., Carrico, I., and Raleigh, D. P. (2010) Modulation of p-cyanophenylalanine fluorescence by amino acid side chains and rational design of fluorescence probes of alpha-helix formation, *Biochemistry 49*, 6290-6295.

[11] Mintzer, M. R., Troxler, T., and Gai, F. (2015) p-Cyanophenylalanine and selenomethionine constitute a useful fluorophore-quencher pair for short distance measurements: application to polyproline peptides, *Phys Chem Chem Phys 17*, 7881-7887.

[12] Yuan, T., Weljie, A. M., and Vogel, H. J. (1998) Tryptophan fluorescence quenching by methionine and selenomethionine residues of calmodulin: orientation of peptide and protein binding, *Biochemistry 37*, 3187-3195.

[13] Peran, I., Watson, M. D., Bilsel, O., and Raleigh, D. P. (2016) Selenomethionine, p-cyanophenylalanine pairs provide a convenient, sensitive, non-perturbing fluorescent probe of local helical structure, *Chem Commun (Camb) 52*, 2055-2058.

[14] Watson, M. D., Peran, I., and Raleigh, D. P. (2016) A Non-perturbing Probe of Coiled Coil Formation Based on Electron Transfer Mediated Fluorescence Quenching, *Biochemistry 55*, 3685-3691.

[15] Sahoo, H., Roccatano, D., Zacharias, M., and Nau, W. M. (2006) Distance distributions of short polypeptides recovered by fluorescence resonance energy transfer in the 10 A domain, *J Am Chem Soc 128*, 8118-8119.

[16] Schaefer, S. A., Dong, M., Rubenstein, R. P., Wilkie, W. A., Bahnson, B. J., Thorpe, C., and Rozovsky, S. (2013) (77)Se enrichment of proteins expands the biological NMR toolbox, *J Mol Biol 425*, 222-231.

[17] Hendrickson, W. A., Horton, J. R., and LeMaster, D. M. (1990) Selenomethionyl proteins produced for analysis by multiwavelength anomalous diffraction (MAD): a vehicle for direct determination of three-dimensional structure, *EMBO J 9*, 1665-1672.

[18] Wu, Y., Kondrashkina, E., Kayatekin, C., Matthews, C. R., and Bilsel, O. (2008) Microsecond acquisition of heterogeneous structure in the folding of a TIM barrel protein, *Proc Natl Acad Sci U S A 105*, 13367-13372.

[19] Chiu, T. K., Kubelka, J., Herbst-Irmer, R., Eaton, W. A., Hofrichter, J., and Davies, D. R. (2005) High-resolution x-ray crystal structures of the villin headpiece subdomain, an ultrafast folding protein, *Proc Natl Acad Sci U S A 102*, 7517-7522.

[20] Hoffman, D. W., Davies, C., Gerchman, S. E., Kycia, J. H., Porter, S. J., White, S. W., and Ramakrishnan, V. (1994) Crystal structure of prokaryotic ribosomal protein L9: a bi-lobed RNA-binding protein, *EMBO J 13*, 205-212.

[21] Guex, N., and Peitsch, M. C. (1997) SWISS-MODEL and the Swiss-PdbViewer: an environment for comparative protein modeling, *Electrophoresis 18*, 2714-2723.

[22] Maier, J. A., Martinez, C., Kasavajhala, K., Wickstrom, L., Hauser, K. E., and Simmerling, C. (2015) ff14SB: Improving the Accuracy of Protein Side Chain and Backbone Parameters from ff99SB, *J Chem Theory Comput 11*, 3696-3713.

[23] Jorgensen, W. L., Chandrasekhar, J., Madura, J. D., Impey, R. W., and Klein, M. L. (1983) Comparison of Simple Potential Functions for Simulating Liquid Water, *J Chem Phys 79*, 926-935.

[24] Darden, T., York, D., and Pedersen, L. (1993) Particle Mesh Ewald - an N.Log(N) Method for Ewald Sums in Large Systems, *J Chem Phys 98*, 10089-10092.

[25] Ryckaert, J. P., Ciccotti, G., and Berendsen, H. J. C. (1977) Numerical-Integration of Cartesian Equations of Motion of a System with Constraints - Molecular-Dynamics of N-Alkanes, *J Comput Phys 23*, 327-341.

[26] Berendsen, H. J. C., Postma, J. P. M., Vangunsteren, W. F., Dinola, A., and Haak, J. R. (1984) Molecular-Dynamics with Coupling to an External Bath, *J Chem Phys 81*, 3684-3690.

[27] Roe, D. R., and Cheatham, T. E., 3rd. (2013) PTRAJ and CPPTRAJ: Software for Processing and Analysis of Molecular Dynamics Trajectory Data, *J Chem Theory Comput 9*, 3084-3095.

[28] Bi, Y., Cho, J. H., Kim, E. Y., Shan, B., Schindelin, H., and Raleigh, D. P. (2007) Rational design, structural and thermodynamic characterization of a hyperstable variant of the villin headpiece helical subdomain, *Biochemistry 46*, 7497-7505.

[29] McKnight, C. J., Matsudaira, P. T., and Kim, P. S. (1997) NMR structure of the 35-residue villin headpiece subdomain, *Nat Struct Biol 4*, 180-184.

[30] Brewer, S. H., Vu, D. M., Tang, Y., Li, Y., Franzen, S., Raleigh, D. P., and Dyer, R. B. (2005) Effect of modulating unfolded state structure on the folding kinetics of the villin headpiece subdomain, *Proc Natl Acad Sci U S A 102*, 16662-16667.

[31] Xiao, S., Patsalo, V., Shan, B., Bi, Y., Green, D. F., and Raleigh, D. P. (2013) Rational modification of protein stability by targeting surface sites leads to complicated results, *Proc Natl Acad Sci U S A 110*, 11337-11342.

[32] Glasscock, J. M., Zhu, Y., Chowdhury, P., Tang, J., and Gai, F. (2008) Using an amino acid fluorescence resonance energy transfer pair to probe protein unfolding: application to the villin headpiece subdomain and the LysM domain, *Biochemistry 47*, 11070-11076.

[33] Kubelka, J., Chiu, T. K., Davies, D. R., Eaton, W. A., and Hofrichter, J. (2006) Sub-microsecond protein folding, *J Mol Biol 359*, 546-553.

[34] Cellmer, T., Henry, E. R., Kubelka, J., Hofrichter, J., and Eaton, W. A. (2007) Relaxation rate for an ultrafast folding protein is independent of chemical denaturant concentration, *J Am Chem Soc 129*, 14564-14565.

[35] Cellmer, T., Buscaglia, M., Henry, E. R., Hofrichter, J., and Eaton, W. A. (2011) Making connections between ultrafast protein folding kinetics and molecular dynamics simulations, *Proc Natl Acad Sci U S A 108*, 6103-6108.

[36] Reiner, A., Henklein, P., and Kiefhaber, T. (2010) An unlocking/relocking barrier in conformational fluctuations of villin headpiece subdomain, *Proc Natl Acad Sci U S A 107*, 4955-4960.

[37] Neumaier, S., and Kiefhaber, T. (2014) Redefining the dry molten globule state of proteins, *J Mol Biol 426*, 2520-2528.

[38] Gelman, H., and Gruebele, M. (2014) Fast protein folding kinetics, *Q Rev Biophys 47*, 95-142.

[39] Brown, J. W., Farelli, J. D., and McKnight, C. J. (2012) On the unyielding hydrophobic core of villin headpiece, *Protein Sci 21*, 647-654.

For Table of Contents Use Only

Selenomethionine Quenching of Tryptophan Fluorescence Provides a Simple Probe of Protein Structure

Matthew D. Watson †, Ivan Peran †, Junjie Zou, Osman Bilsel and Daniel P. Raleigh

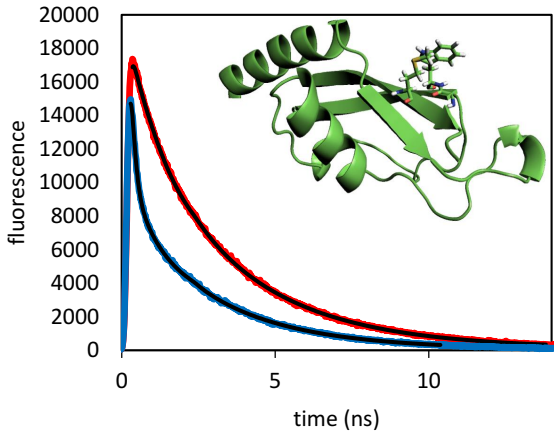

SUPPORTING INFORMATION FOR

Selenomethionine Quenching of Tryptophan Fluorescence Provides a Simple Probe of Protein Structure

Matthew D. Watson†, Ivan Peran†, Junjie Zou, Osman Bilsel and Daniel P. Raleigh*

†These authors contributed equally to this work

*Person to whom correspondence should be addressed

Estimation of Helical Content

The percent of helical structure in the 21 residue helical peptide was calculated from the molar ellipticity at 222 nm, $[\theta]_{obs}$ using the the expression

$$f_h = \frac{[\theta]_{obs} - [\theta]_C}{[\theta]_H - [\theta]_C} \quad \text{(S1)}$$

Where $[\theta]_H$ is the molar ellipticity at 222 nm for a 100% helical peptide and $[\theta]_C$ is the molar ellipticity at 222 nm for a random coil:

$$[\theta]_H = -40000\left(1 - \frac{2.5}{n}\right) + 100T \quad \text{(S2)}$$

$$[\theta]_C = 640 - 45T \quad \text{(S3)}$$

Where *n* is the number of residues in the peptide and *T* is the temperature in °C.[1]

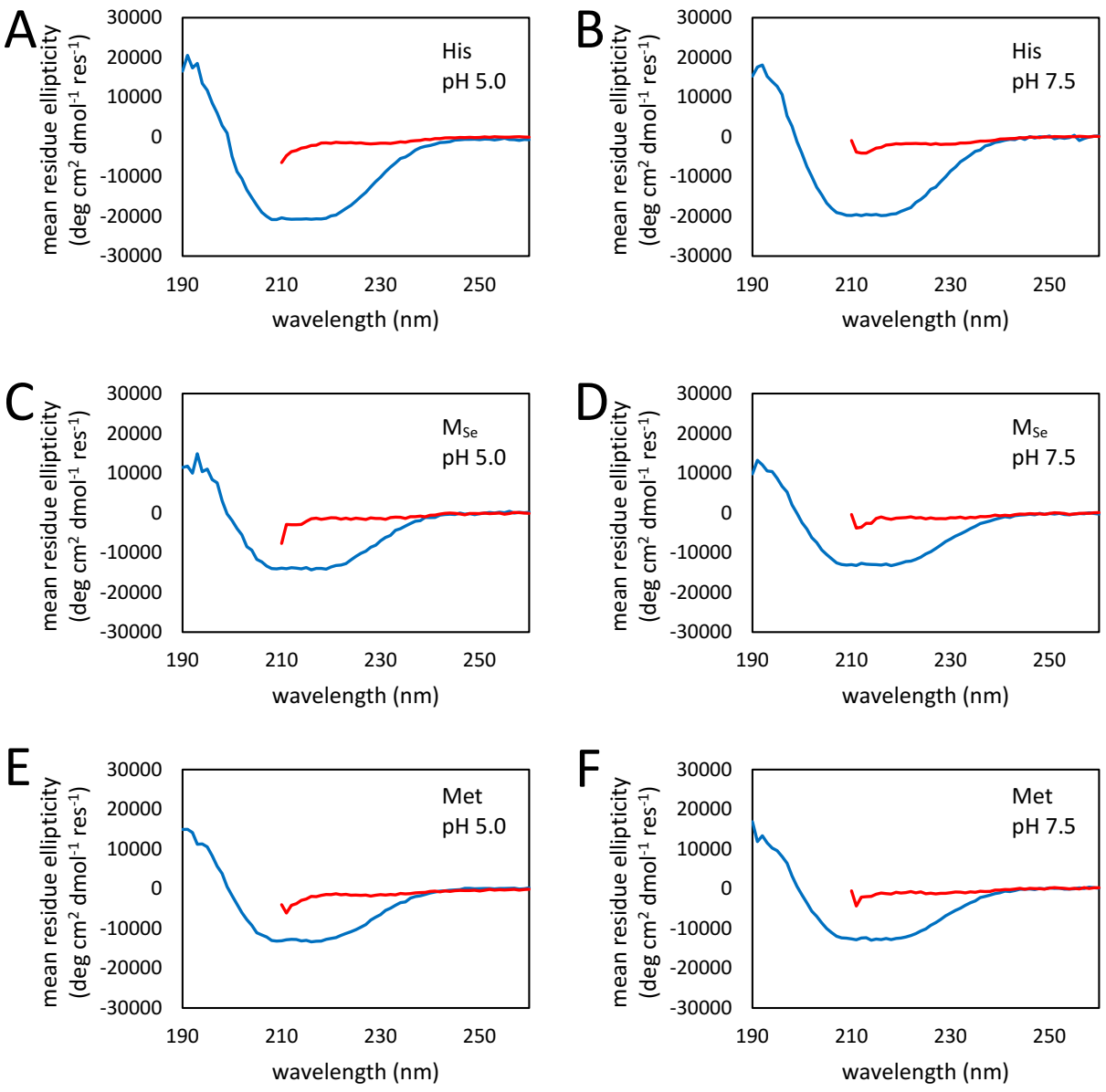

Figure S1: (A) CD spectra of Y126W-CTL9 at 20 °C in 20 mM acetate buffer at pH 5.0 (blue) and in the same buffer with 9.5 M urea (red). **(B)** CD spectra of Y126W-CTL9 at 20 °C in 20 mM tris buffer at pH 7.5 (blue) and in the same buffer with 9.5 M urea (red). **(C)** CD spectra of Y126W/H144M_{Se}-CTL9 at 20 °C in 20 mM acetate buffer at pH 5.0 (blue) and in the same buffer with 9.5 M urea (red). **(D)** CD spectra of Y126W/H144M_{Se}-CTL9 at 20 °C in 20 mM tris buffer at pH 7.5 (blue) and in the same buffer with 9.5 M urea (red). **(E)** CD spectra of Y126W/H144M-CTL9 at 20 °C in 20 mM acetate buffer at pH 5.0 (blue) and in the same buffer with 9.5 M urea (red). **(F)** CD spectra of Y126W/H144M-CTL9 at 20 °C in 20 mM tris buffer at pH 7.5 (blue) and in the same buffer with 9.5 M urea (red). The protein concentration in all samples was 25 µM.

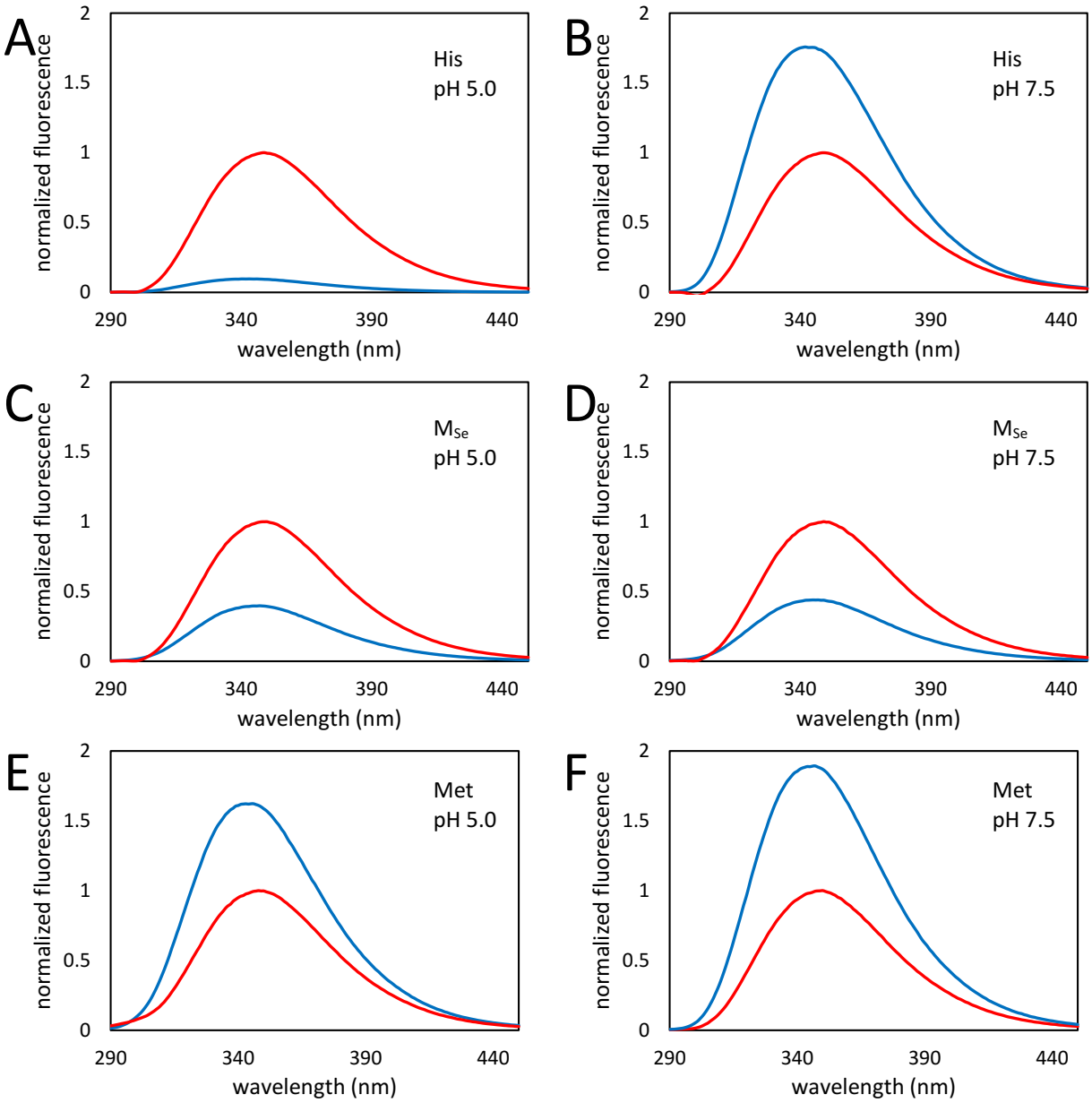

Figure S2: (A) Fluorescence emission spectra of Y126W-CTL9 at 20 °C in 20 mM acetate buffer at pH 5.0 (blue) and in the same buffer with 9.5 M urea (red). **(B)** Fluorescence emission spectra of Y126W-CTL9 at 20 °C in 20 mM tris buffer at pH 7.5 (blue) and in the same buffer with 9.5 M urea (red). **(C)** Fluorescence emission spectra of Y126W/H144M_{Se}-CTL9 at 20 °C in 20 mM acetate buffer at pH 5.0 (blue) and in the same buffer with 9.5 M urea (red). **(D)** Fluorescence emission spectra of Y126W/H144M_{Se}-CTL9 at 20 °C in 20 mM tris buffer at pH 7.5 (blue) and in the same buffer with 9.5 M urea (red). **(E)** Fluorescence emission spectra of Y126W/H144M-CTL9 at 20 °C in 20 mM acetate buffer at pH 5.0 (blue) and in the same buffer with 9.5 M urea (red). **(F)** Fluorescence emission spectra of Y126W/H144M-CTL9 at 20 °C in 20 mM tris buffer at pH 7.5 (blue) and in the same buffer with 9.5 M urea (red). Note that panels **(B)**, **(D)** and **(F)** are included in Figure 1 of the manuscript and are reproduced here for clarity. The protein concentration in all samples was 25 µM.

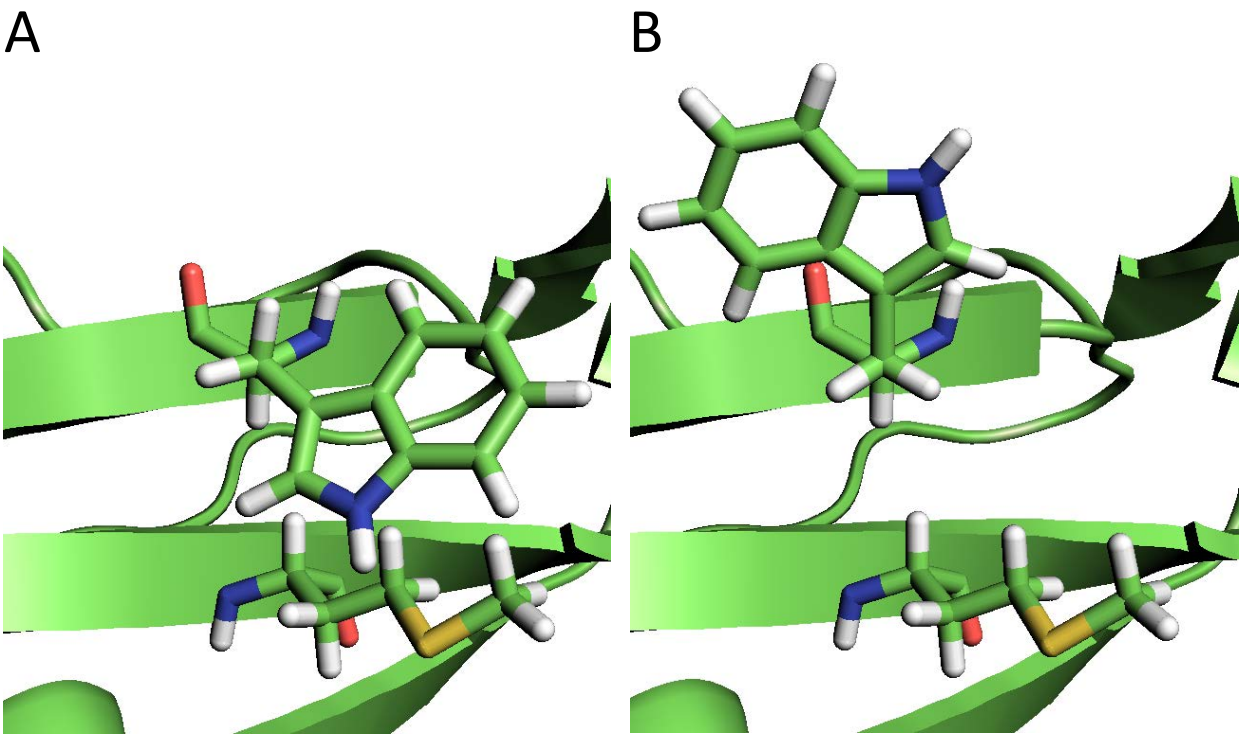

Figure S3: Models of the allowed χ_1 rotamers for Y126W/H144M_{Se}-CTL9 based on PDB structure 1DIV.[2] **(A)** The $\chi_1 \approx -60°$ rotamer, which corresponds to the orientation of the phenol ring of Tyr in the crystal structure, packing the indole ring against the M_{Se} sidechain. **(B)** The $\chi_1 \approx 60°$ rotamer, which exposes the Trp sidechain to solvent and moves the indole ring out of van der Waals contact with the Se atom.

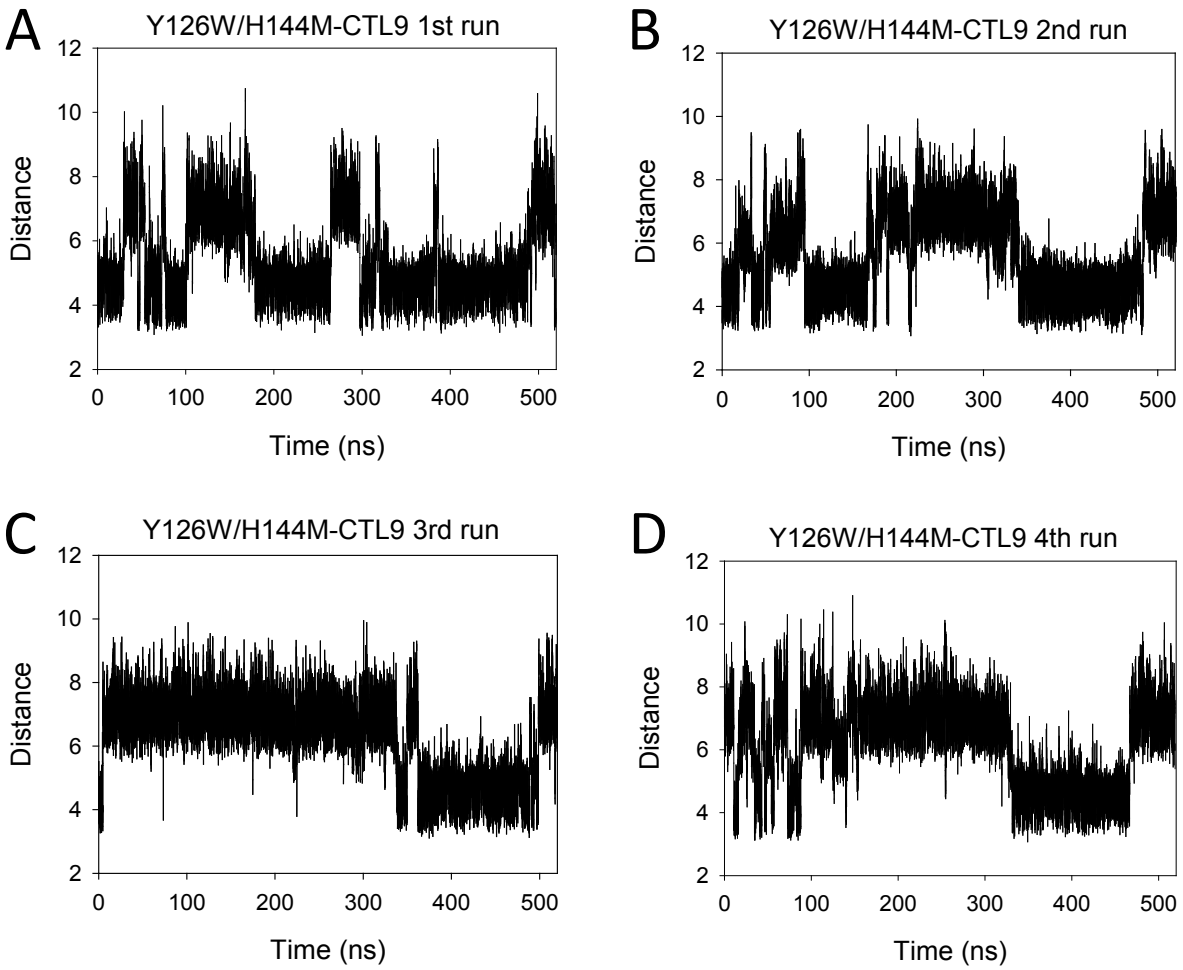

Figure S4. Distance in Å between the geometric center of Cδ2 and Cε2 of the Trp indole ring and sulfur atom of Met during the MD simulations of Y126W/H144M-CTL9. **(A)** and **(B)** Independent MD simulations in which W126 starts with the rotamer χ_1 = -65.0°, χ_2 = -84.9° **(C)** MD simulation in which W126 starts with the rotamer χ_1 = -71.2°, χ_2 = 94.3° **(D)** MD simulation in which W126 starts with the rotamer χ_1 = 62.1°, χ_2 = 94.4°

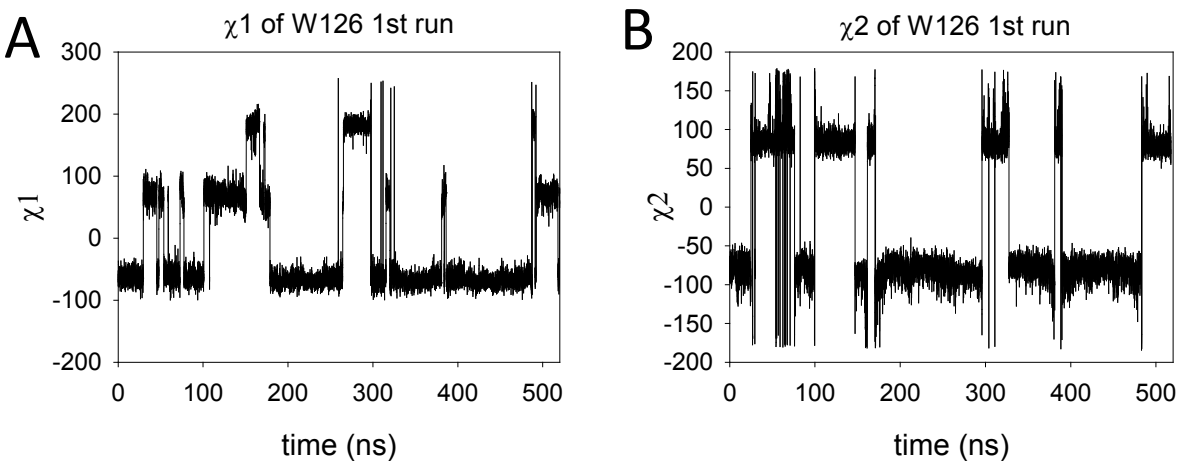

Figure S5. The χ_1 and χ_2 dihedral angles of W126 in Y126W/H144M-CTL9 during the 1st run of the MD simulations in which W126 starts with a rotamer state of χ_1 = -65.0°, χ_2 = -84.9° **(A)** The χ_1 angle of W126 in degrees *vs* time. **(B)** The χ2 angle of W126 in degrees *vs* time.

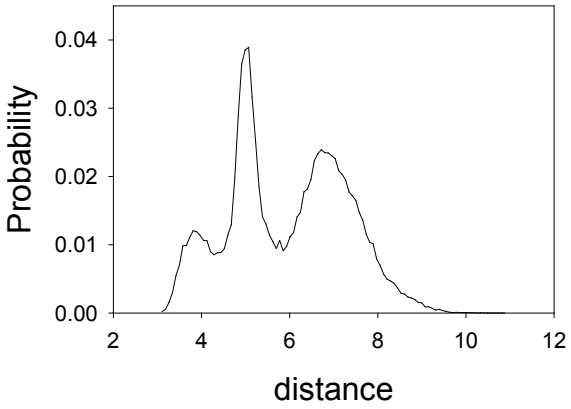

Figure S6. A histogram showing the distribution of the distances between W126 and M144 in Y126W/H144M-CTL9 collected from all 4 MD simulations. The distance was measured between the geometric center of Cδ2 and Cε2 of the Trp indole ring and the sulfur atom of Met.

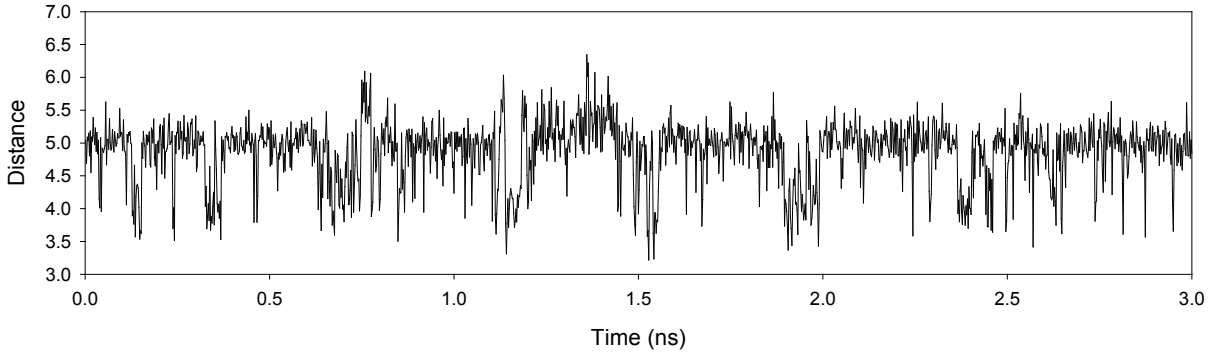

Figure S7. The distance between W126 and M144 of Y126W/H144M-CTL9 during a 3 ns MD simulation with a sampling frequency of 0.002 ns.

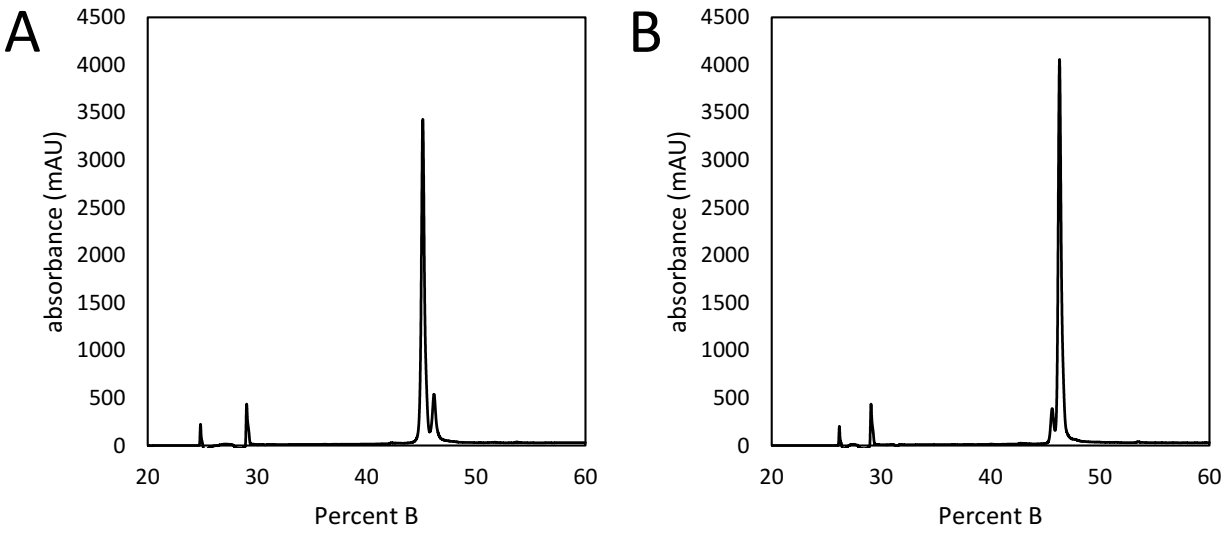

Figure S8. Selenomethionine is efficiently oxidized by 0.005% H_2O_2 while methionine is not. **(A)** Preparative HPLC trace of Y126W/H144M_{Se}-CTL9 after oxidation in 0.005% H_2O_2 for 4 hr. The peak centered at 45% B was identified by LC-ESI-TOF MS as Y126W/H144M_{SeO}-CTL9 and the peak centered at 46% B was identified as Y126W/H144M_{Se}-CTL9. **(B)** Preparative HPLC trace of Y126W/H144M-CTL9 after oxidation in 0.005% H_2O_2 for 4 hr. The peak centered at 46% B was identified by LC-ESI-TOF MS as Y126W/H144M_{ox}-CTL9 and the peak centered at 47% B was identified as Y126W/H144M-CTL9. The absorbance was monitored at 220 nm.

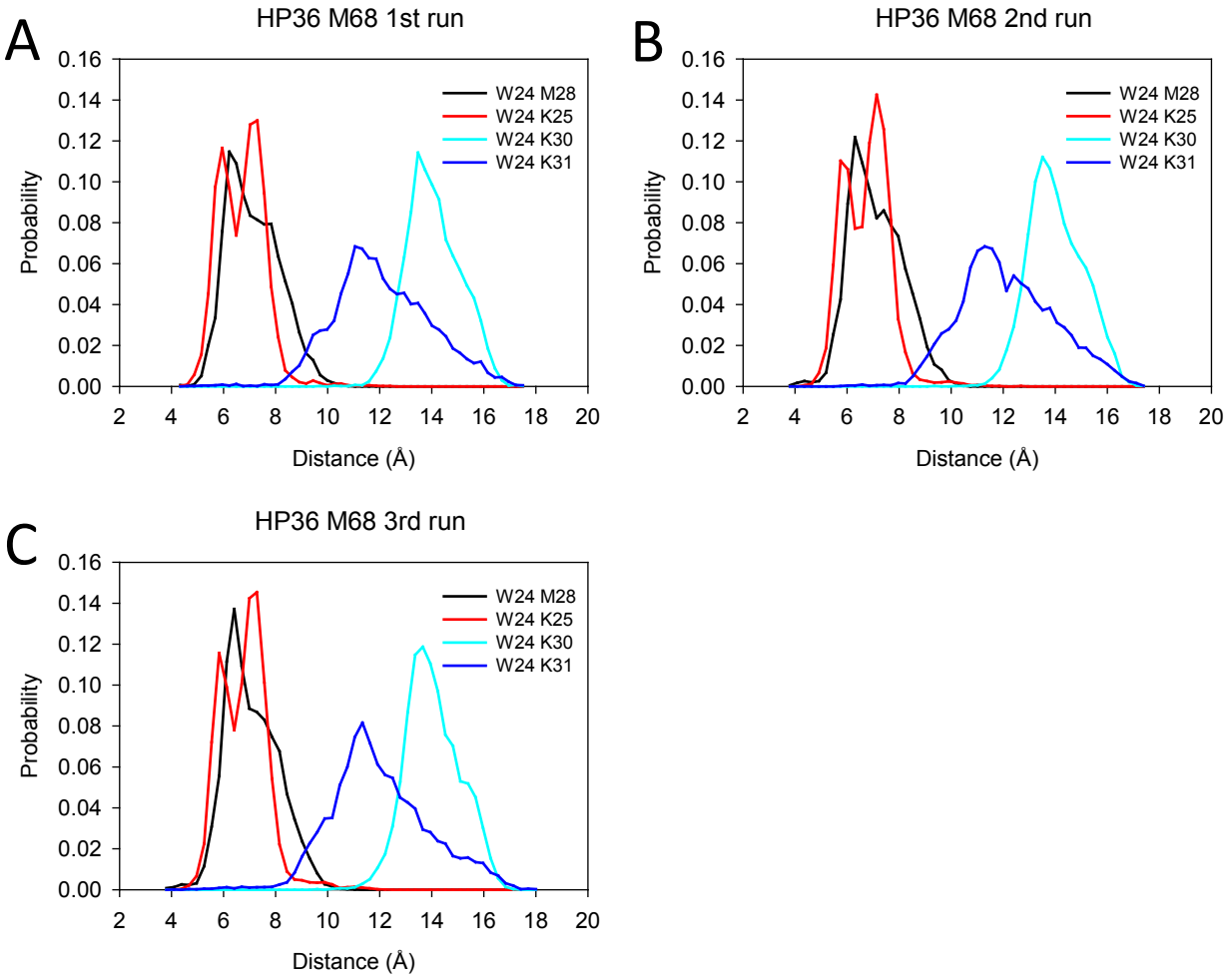

Figure S9. Distribution of distances between W24/M28, W24/K25, W24/K30 and W24/K31 in N28M-HP36 from the last 300 ns of three independent 400 ns MD simulations, which used starting structures with different rotamer states of W24. **(A)** χ_1 = 63.2°, χ_2 = 85.5° **(B)** χ_1 = -82.2°, χ_2 = -89.3° **(C)** χ_1 = -177.0°, χ_2 = 75.0°

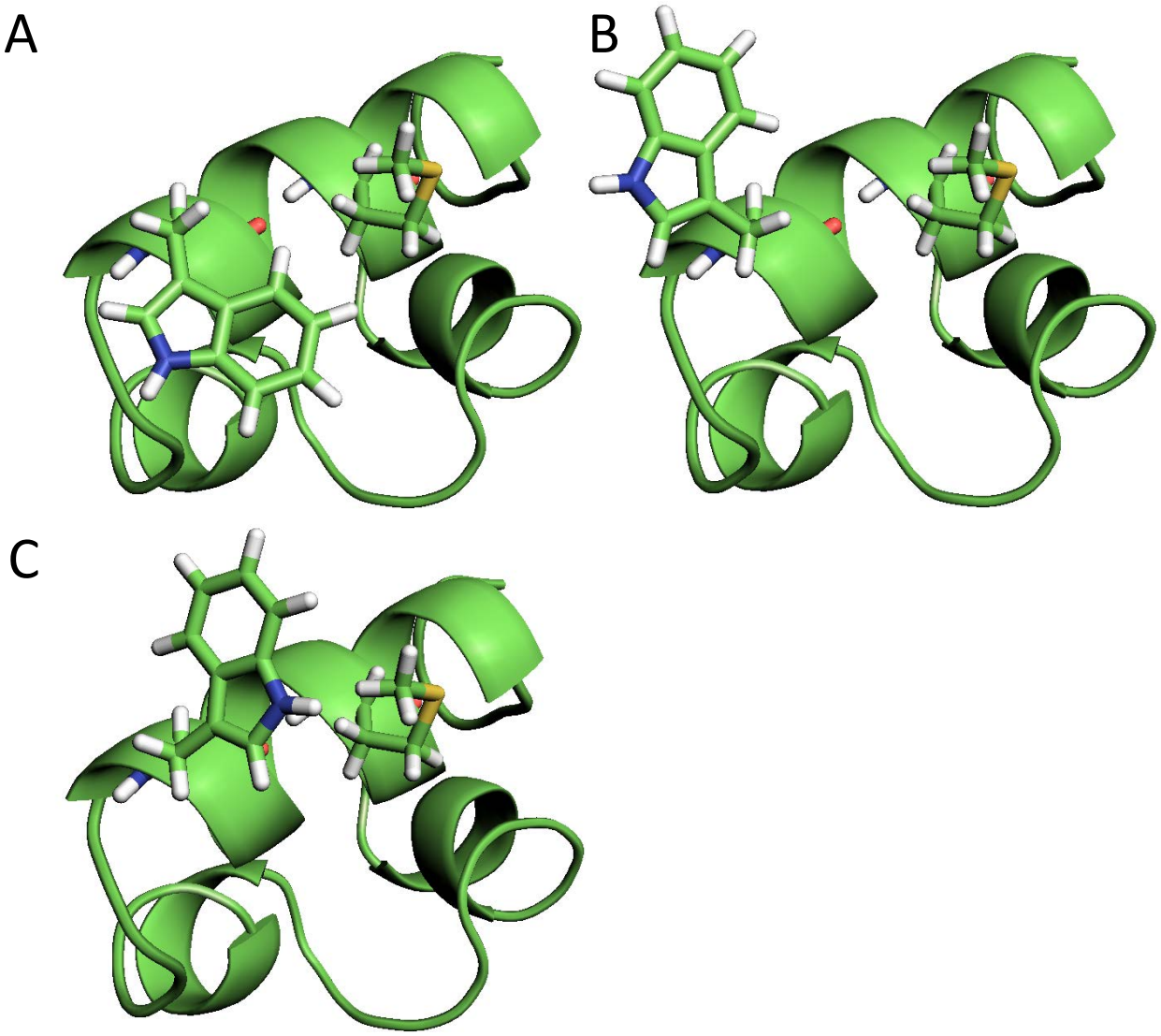

Figure S10: Models of the allowed χ_1 rotamers for N28M_{Se}-HP36 based on PDB structure 1VII.[3] **(A)** The $\chi_1 \approx 60°$ rotamer, the orientation from the crystal structure, which may bring the indole ring into transient contact with the Se atom. **(B)** The $\chi_1 \approx -60°$ rotamer, which exposes the Trp sidechain to solvent and moves the indole ring out of van der Waals contact with the Se atom. **(C)** The $\chi_1 \approx 180°$ rotamer, which brings the indole ring into close contact with the Se atom.

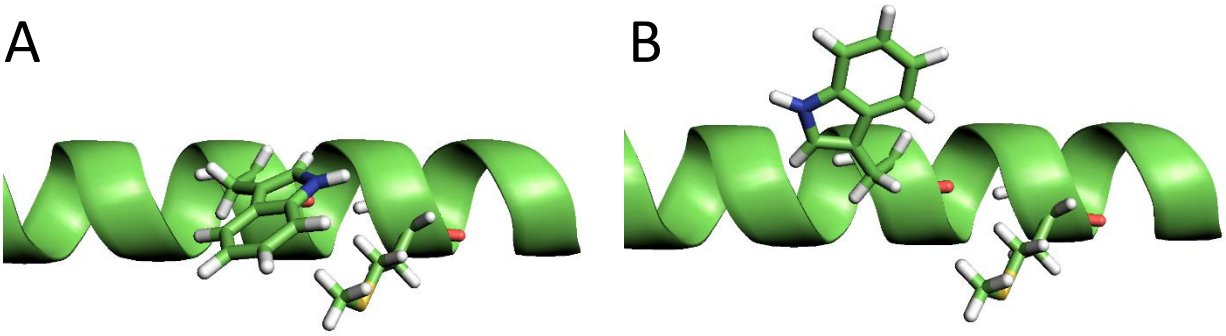

Figure S11: Models of the allowed χ_1 rotamers for the 21 residue helical peptide. **(A)** The $\chi_1 \approx 180°$ rotamer, which brings the indole ring into close contact with the Se atom. **(B)** The $\chi_1 \approx -60°$ rotamer, which moves the indole ring out of van der Waals contact with the Se atom.

Supporting References

[1] Kuhlman, B., Yang, H. Y., Boice, J. A., Fairman, R., and Raleigh, D. P. (1997) An exceptionally stable helix from the ribosomal protein L9: implications for protein folding and stability, *J Mol Biol 270*, 640-647.

[2] Hoffman, D. W., Davies, C., Gerchman, S. E., Kycia, J. H., Porter, S. J., White, S. W., and Ramakrishnan, V. (1994) Crystal structure of prokaryotic ribosomal protein L9: a bi-lobed RNA-binding protein, *EMBO J 13*, 205-212.

[3] McKnight, C. J., Matsudaira, P. T., and Kim, P. S. (1997) NMR structure of the 35-residue villin headpiece subdomain, *Nat Struct Biol 4*, 180-184.